Supplementary Information:

Synergistically optimizing interdependent thermoelectric parameters of *n*-type PbSe through alloying CdSe

Xin Qian,[1,‡] Haijun Wu,[2,‡] Dongyang Wang,[1,‡] Yang Zhang,[2] Jinfeng Wang,[3] Guangtao Wang,[3] Lei Zheng,[1,*] Stephen J. Pennycook,[2] Li-Dong Zhao[1,*]

[1]*School of Materials Science and Engineering, Beihang University, Beijing 100191, China.*

[2]*Department of Materials Science and Engineering, National University of Singapore, 7 Engineering Drive 1, Singapore 117575, Singapore.*

[3]*College of Physics and Materials Science, Henan Normal University, Xinxiang, 453007, China*

‡ These authors contributed equally to this work.

*Corresponding authors: zhenglei@buaa.edu.cn; zhaolidong@buaa.edu.cn

1. Experimental details:

Samples preparation: High-purity raw materials, Pb chunk (99.999%, Aladdin, China), Se chunk (99.999%, Aladdin, China), Cd shot (99.99%) and Sb shot (99.999%, Aladdin, China), were weighed and loaded into silica tubes under an N_2-filled glovebox according to the nominal compositions of PbSe-*x*%CdSe (mol fraction in the text, x = 0, 1, 2, 3 and 4), all the samples are doped with 1% Sb to optimize carrier concentration. Then, the tubes were flame-sealed under vacuum (below ~10^{-4} Torr) and slowly heated to 1423 K with 24 h, soaked at this temperature for 12 h and subsequently cooled to room temperature in the furnace. The obtained ingots were ground into fine powder and densified by spark plasma sintering (SPS-211LX, Fuji Electronic Industrial Co., Ltd.) at 873 K for 5 min under an axial compressive stress of 50 MPa. Highly densified (> 95% of theoretical density) disk-shaped pellets with dimensions of Φ15 mm × 9 mm were obtained.

Band gap measurements: The optical band gap measurements were carried out on the finely ground powders using Infrared Diffuse Reflection method with a Fourier Transform Infrared Spectrometer (IRAffinity-1S). The spectra were collected in the mid-IR range (5000 ~ 450 cm^{-1}) and the reflectance versus wavelength data generated. The band gap was estimated by converting reflectance to absorption data according to Kubelka-Munk equations: $\alpha/S = (1-R)^2/(2R)$, where R is the reflectance, α and S are the absorption and scattering coefficients, respectively.

Electrical transport properties: The obtained SPS-processed pellets were cut into bars with dimensions of 3 × 3 × 12 mm^3 for simultaneous measurement of the electrical resistivity and Seebeck coefficient using a CTA instrument (Cryoall, China) under a helium atmosphere from room temperature to 873 K. The bars were coated with a thin layer of boron nitride (BN) to protect instruments. The uncertainty of the Seebeck coefficient and electrical resistivity measurements is 5%.

Hall measurements: Room temperature Hall coefficients (R_H) were measured under a reversible magnetic field (0.9 T) by the Van der Pauw method by using a Hall measurement system (Lake Shore 8400 Series, Model 8404, USA). Carrier

concentration (n_H) is obtained by n_H = 1/ (e·R_H), and carrier mobility (μ_H) is calculated using the relationship $\mu_H = \sigma \cdot R_H$ with σ being the electrical conductivity obtained from the CTA instrument.

Thermal transport properties: The obtained SPS-processed pellets were cut into thin square pieces with dimensions of 8 × 8 mm and 1~2 mm in thickness for the measurement of thermal diffusivity (D) using a laser flash diffusivity method (LFA457, Netzsch, Germany). The samples were coated with a thin layer of graphite to minimize errors from the material emissivity. The thermal conductivity was calculated as $\kappa = D \cdot \underline{C}_p \cdot \rho$, where D is the thermal diffusivity coefficient analyzed using a Cowan model with pulse correction, C_p is the specific heat capacity estimated with Dulong-Petit Law[1], and the sample density (ρ) was determined using the dimensions and mass of the sample. The uncertainty of the thermal conductivity is estimated to be within 10%, comprising uncertainties of 3% for the thermal diffusivity (D), 5% for the specific heat (C_p), and 2% for the sample density (ρ). The combined uncertainty for all measurements involved in the calculation of ZT is around 20%.

X-ray diffraction and Electron microscopy: Samples pulverized with an agate mortar were used for powder X-ray diffraction (XRD). The XRD powder diffraction patterns for all samples were collected using a D/max 2500PC X-ray diffractometer with Cu Kα (λ = 1.5418 Å) radiation in a reflection geometry on an Inel diffractometer operating at 40 KV and 20 mA and equipped with a position-sensitive detector. (Scanning) transmission electron microscopy (STEM/TEM) investigations were carried out in a JEOL ARM200F atomic resolution analytical electron microscope operated at 200 kV. The thin TEM specimens were prepared by conventional methods, the procedures were performed including the cutting, grinding, dimpling, polishing and Ar-ion milling in a liquid nitrogen environment.

Band structure calculations: First-principles calculations within density functional theory (DFT) have been carried out for $Pb_{27}Se_{27}$, $Pb_{63}CdSe_{64}$ and $Pb_{26}CdSe_{27}$ using the projector-augmented wave (PAW) method[2, 3] as implemented in the Vienna Ab-initio Simulation Package (VASP).[4] The PBEsol exchange-correlation functional was used to model crystal and electronic structure.[5] The electronic valence

configurations for Pb, Cd and Se are $5d^{10}6s^26p^2$, $4d^{10}5s^2$ and $4s^24p^4$, respectively. The Kohn-Sham orbitals are expanded in plane waves with a kinetic energy cutoff of 500 eV. The 3 × 3 × 3 supercell based on rock-salt primitive cell of PbSe was adopted to evaluate the electronic structure of pure ($Pb_{27}Se_{27}$) and Cd alloyed ($Pb_{63}CdSe_{64}$, $Pb_{26}CdSe_{27}$). All the structures are fully relaxed until the maximum residual ionic force is below 0.01 eV/Å, and the total energy difference is converged to within 10^{-6} eV.

2. Callaway model calculation

In a solid solution system, point defects scattering derives from both the mass fluctuations and the size and the strain field fluctuations between the impurity atom and the host lattice. Callaway model[1, 6, 7] has been applied to describe the influence of point defects on the lattice thermal conductivity. Here we present a phonon scattering model on the basis of the above theory and try to describe the effect of CdSe alloying on the lattice thermal conductivity of PbSe.

At temperatures above the Debye temperature, if the effects on lattice thermal conductivity mainly results from point defects scattering, the ratio of the lattice thermal conductivity of a material (κ_{lat}) to that of the parent material ($\kappa_{lat,\,p}$) can be described in the following equation:[1, 7]

$$\frac{\kappa_{lat}}{\kappa_{lat,p}} = \frac{tan^{-1}(U)}{U} \tag{1}$$

where the parameter U is defined as follows:[7, 8]

$$U = \left(\frac{\pi^2 \Theta_D \Omega}{h v_a^2} \kappa_{lat,p} \Gamma\right)^{1/2} \tag{2}$$

where h, v_a, Θ_D, Ω and Γ stand for the Planck constant, average sound velocity, Debye temperature, average volume per atom and imperfection scaling parameter. The average sound velocity (v_a) is calculated through the following formula:[1, 7]

$$v_a = \left[\frac{1}{3}\left(\frac{1}{v_l^3} + \frac{2}{v_s^3}\right)\right]^{-1/3} \tag{3}$$

where the longitudinal (v_l) and transverse (v_s) sound velocities are experimentally

measured and listed in Table 2. The Debye temperature (Θ_D) is defined by:[7]

$$\Theta_D = \frac{h}{k_B}\left(\frac{3N}{4\pi V}\right)^{1/3} v_a \tag{4}$$

where the V is the unit-cell volume, N is the number of atoms in a unit cell, k_B is the Boltzmann parameter, and h presents the Planck constant. The imperfection scaling parameter Γ includes two components: the mass fluctuations Γ_M and the strain field fluctuations Γ_S. Generally, the imperfection scaling parameter can write $\Gamma = \Gamma_M + \varepsilon\,\Gamma_S$, where ε is a phenomenological adjustable parameter because of the uncertainty of Γ_S.[1, 7] In this work, ε is calculated by the following equations:[6, 7, 9]

$$\varepsilon = \frac{2}{9}\left(\frac{6.4 \times \gamma(1+\upsilon_p)}{1-\upsilon_p}\right)^2 \tag{5}$$

where υ_p is the Poisson ratio, which can be derived from the longitudinal (v_l) and transverse (v_s) sound velocities by the relationship as:[6, 7, 9]

$$\upsilon_p = \frac{1 - 2\left(v_s / v_l\right)^2}{2 - 2\left(v_s / v_l\right)^2} \tag{6}$$

Grüneisen parameter (γ) is calculated using Poisson ratio (υ_p) as:[6, 7, 9]

$$\gamma = \frac{3}{2}\left(\frac{1+\upsilon_p}{2-3\upsilon_p}\right) \tag{7}$$

Since the Se site has no change when Cd atom substitutes the Pb site, $\Gamma_{Se} = 0$. Therefore, the imperfection scaling parameter can be defined as follows:[1, 7]

$$\Gamma_{Pb_{1-x}Cd_xSe} = \frac{1}{2}\left(\frac{M_{(Pb,Cd)}}{\bar{M}}\right)^2 \Gamma_{(Pb,Cd)} \tag{8}$$

where $\bar{M} = \dfrac{M_{Pb} + M_{Cd}}{2}$

$$\Gamma_{(Pb,Cd)} = \Gamma_{M,(Pb,Cd)} + \varepsilon\Gamma_{S,(Pb,Cd)} \tag{9}$$

$$\Gamma_{M,\ (Pb,Cd)} = x(1-x)\left(\frac{\Delta M}{M_{(Pb,Cd)}}\right)^2 \tag{10}$$

where $\Delta M = M_{Pb} - M_{Cd}$ and $M_{(Pb,Cd)} = (1-x)M_{Pb} + xM_{Cd}$

$$\Gamma_{S,\ (Pb,Cd)} = x(1-x)\left(\frac{\Delta r}{r_{(Pb,Cd)}}\right)^2 \tag{11}$$

where $\Delta r = r_{Pb} - r_{Cd}$ and $r_{(Pb,Cd)} = (1-x)r_{Pb} + xr_{Cd}$

then, $$\Gamma_{Pb_{1-x}Cd_xSe} = \frac{1}{2}\left(\frac{M_{(Pb,Cd)}}{\bar{M}}\right)^2 x(1-x)\left[\left(\frac{\Delta M}{M_{(Pb,Cd)}}\right)^2 + \varepsilon\left(\frac{\Delta r}{r_{(Pb,Cd)}}\right)^2\right] \tag{12}$$

References

1 Y. Xiao, W. Li, C. Chang, Y. Chen, L. Huang, J. Q. He and L.-D. Zhao, *J. Alloys Compd.*, 2017, **724**, 208-221.

2 P. E. Blöchl, *Phys. Rev. B*, 1994, **50**, 17953-17979.

3 G. Kresse and D. Joubert, *Phys. Rev. B*, 1999, **59**, 1758-1775.

4 G. Kresse and J. Furthmüller, *Phys. Rev. B*, 1996, **54**, 11169-11186.

5 L. A. Constantin, J. M. Pitarke, J. F. Dobson, A. Garcia-Lekue and J. P. Perdew, *Phys. Rev. Lett.*, 2008, **100**, 036401.

6 J. Callaway and H. C. von Baeyer, *Phys. Rev.*, 1960, **120**, 1149-1154.

7 Y.-L. Pei, J. Q. He, J.-F. Li, F. Li, Q. Liu, W. Pan, C. Barreteau, D. Berardan, N. Dragoe and L.-D. Zhao, *Npg Asia Mater.*, 2013, **5**, e47.

8 Y. Xiao, H. J. Wu, J. Cui, D. Y. Wang, L. W. Fu, Y. Zhang, Y. Chen, J. Q. He, S. J. Pennycook and L.-D. Zhao, *Energy Environ. Sci.*, 2018, **11**, 2486-2495.

9 G. J. Tan, F. Y. Shi, H. Sun, L.-D. Zhao, C. Uher, V. P. Dravid and M. G. Kanatzidis, *J. Mater. Chem. A*, 2014, **2**, 20849-20854.

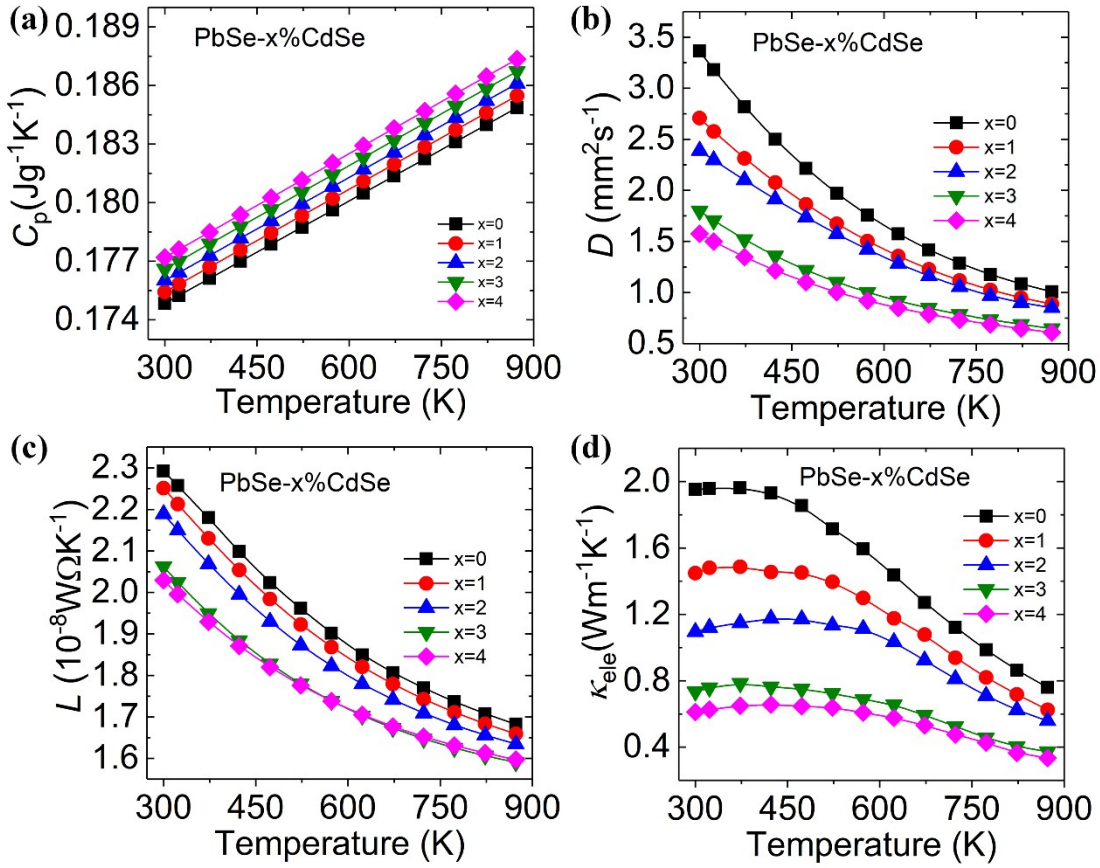

Fig. S1 (a) Specific heat, (b) Thermal diffusivity, (c) Lorenz number and (d) Electronic thermal conductivity of PbSe-CdSe.

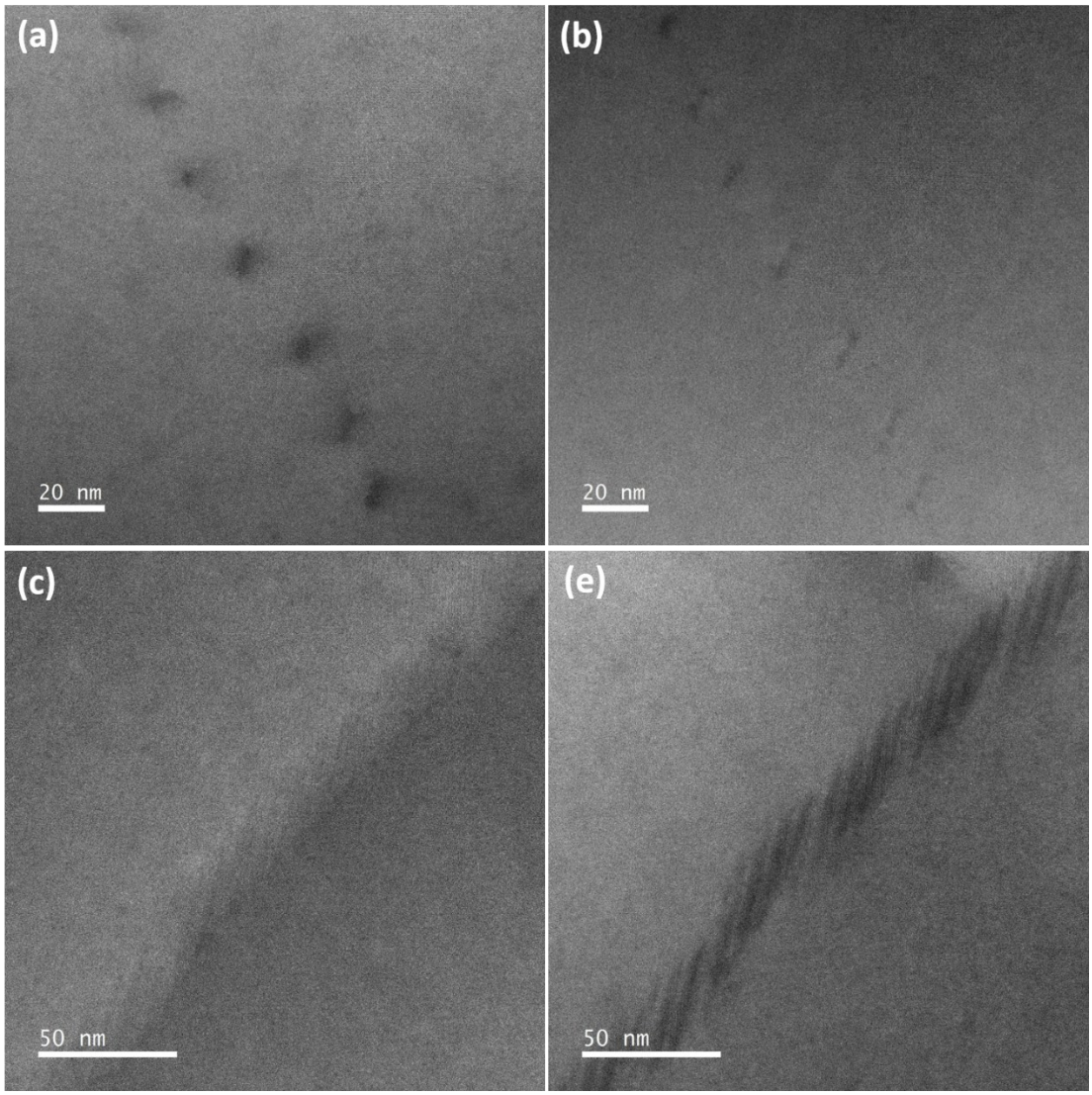

Fig. S2 Arrayed line defects inside grains. (a, b) and (c, d) Simultaneously acquired STEM HAADF and ABF images.

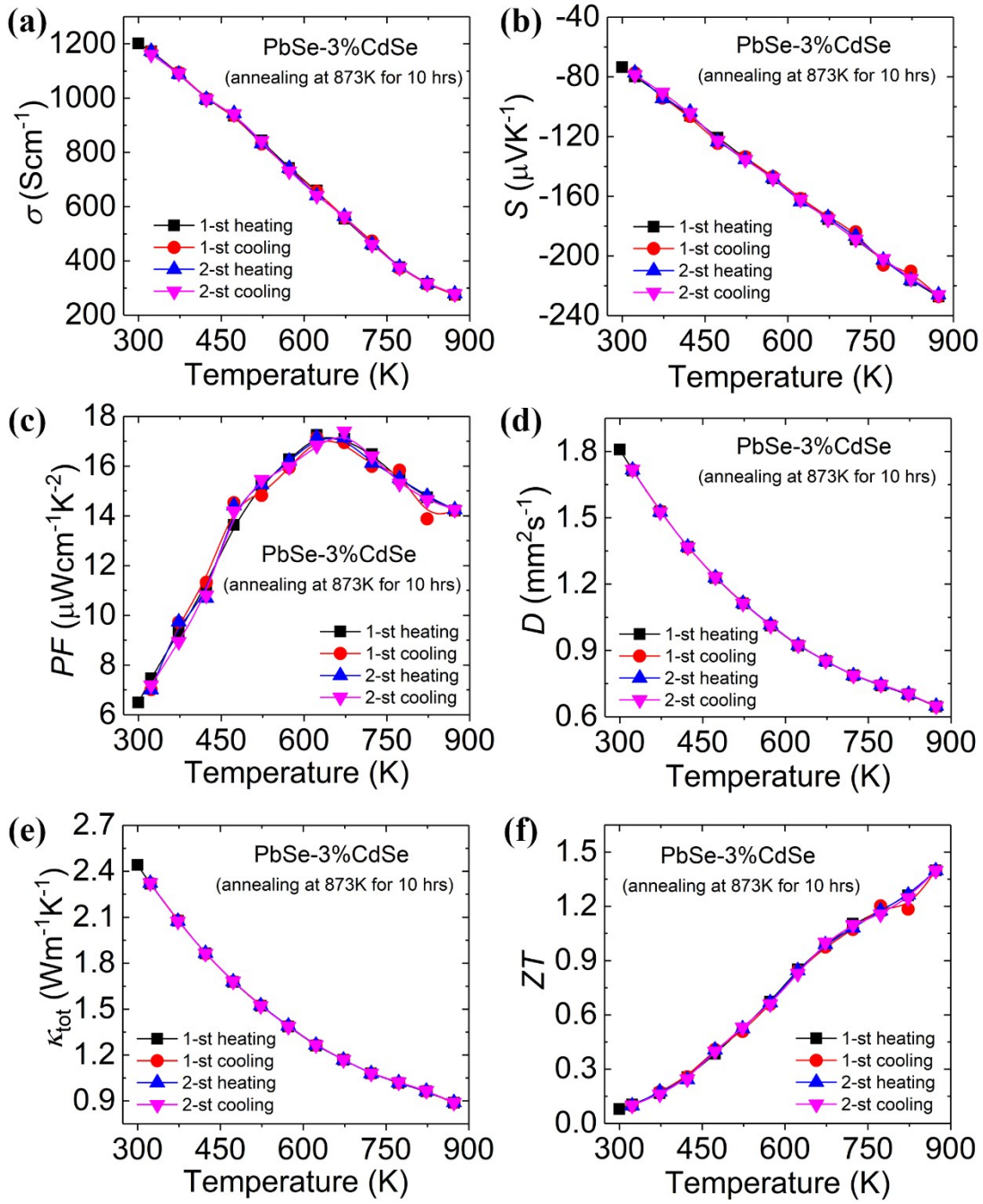

Fig. S3 Thermoelectric transport properties of PbSe-3%CdSe annealed at 873K for 10 hours: (a) electrical conductivity, (b) Seebeck coefficient, (c) power factor, (d) thermal diffusivity, (e) total thermal conductivity and (f) *ZT* value.

Table S1. Density of samples in the work

Composition	Theoretical Density, (g/cc)	Measured Density, (g/cc)	Theoretical Density, (%)
PbSe	8.150	7.876	96.64
PbSe-1%CdSe	8.127	8.024	98.74
PbSe-2%CdSe	8.103	7.822	96.53
PbSe-3%CdSe	8.080	7.802	96.56
PbSe-4%CdSe	7.882	7.608	96.52